Axial-Vector D_1 Hadrons in $D^*\pi$ Scattering from QCD

Nicolas Lang[1,*] and David J. Wilson[2,†]

(for the Hadron Spectrum Collaboration)

[1]School of Mathematics, Trinity College, Dublin 2, Ireland
[2]DAMTP, University of Cambridge, Centre for Mathematical Sciences, Wilberforce Road, Cambridge CB3 0WA, United Kingdom

(Received 24 May 2022; accepted 20 October 2022; published 15 December 2022)

We present $I = 1/2$ $D^*\pi$ scattering amplitudes from lattice QCD and determine two low-lying $J^P = 1^+$ axial-vector D_1 states and a $J^P = 2^+$ tensor D_2^*. Computing finite-volume spectra at a light-quark mass corresponding to $m_\pi \approx 391$ MeV, for the first time, we are able to constrain coupled $J^P = 1^+$ $D^*\pi$ amplitudes with $^{2S+1}\ell_J = {}^3S_1$ and ${}^3D_1$ as well as coupled $J^P = 2^+$ $D\pi({}^1D_2\}$ and $D^*\pi({}^3D_2\}$ amplitudes via Lüscher's quantization condition. Analyzing the scattering amplitudes for poles we find a near-threshold bound state, producing a broad feature in $D^*\pi\{{}^3S_1\}$. A narrow bump occurs in $D^*\pi\{{}^3D_1\}$ due to a D_1 resonance. A single resonance is found in $J^P = 2^+$ coupled to $D\pi$ and $D^*\pi$. A relatively low mass and large coupling are found for the lightest D_1, suggestive of a state that will evolve into a broad resonance as the light-quark mass is reduced. An earlier calculation of the scalar D_0^* using the same light-quark mass enables comparisons to the heavy-quark limit.

DOI: 10.1103/PhysRevLett.129.252001

Introduction.—Since their discovery, the lightest scalar D-meson excitations have raised questions about their mass ordering, widths, and composition. Heavy-quark spin symmetry suggests the same questions apply to the axial vectors. At the same time, the D-meson resonances are exemplary for several charmed states [1–4], some manifestly exotic, arising in coupled-channel systems and close to thresholds. They may therefore serve as a place to obtain a more general understanding of QCD dynamics among charmed hadrons.

In experiment, there are four low-lying positive-parity D-mesons [5]: a scalar $D_0^*(2300)$, two axial vectors $D_1(2430)$ and $D_1(2420)$, and a tensor $D_2^*(2460)$. The scalar and $D_1(2430)$ are very broad and are thought to couple strongly to their respective $D\pi$ and $D^*\pi$ decay modes. The $D_1(2420)$ and the tensor D_2^* are relatively narrow, the D_2^* decaying into both $D\pi$ and $D^*\pi$.

Several theoretical approaches have been applied to understand these states. Quark potential models [6] provide a useful qualitative starting point leading to four states arising from the $\ell = 1$ singlet ${}^1P_1$ and triplet ${}^3P_J$ combinations. Charge conjugation is not a good symmetry so ${}^1P_1$ and ${}^3P_1$ mix. This produces one $J^P = 0^+$, two 1^+, and a 2^+ state at similar masses [6]. Approaches accounting for the presence of decay channels [7–12] are necessary when strong S-wave decay modes are present. Recent studies have shown that the scalar D_0^* pole may be far below its currently reported value [8,13–18], and the same could be true of the broad D_1 [10,19].

One particularly useful theoretical perspective is obtained by considering the behavior when the charm quark becomes infinitely heavy with respect to both the light quarks and the scale of QCD interactions [7,14,20–25]. In this limit the spin of the heavy quark is conserved, and the D-meson states can be characterized by the vector sum of the orbital angular momentum and the light-quark spin. For the quark-model $\ell = 1$ states two doublets arise. One doublet contains the D_0^* and one of the D_1 mesons, and in the infinitely heavy-quark limit they decay exclusively via S-wave interactions. The other contains a D_1 and the D_2^* decaying entirely by D-wave interactions.

Recent advances have enabled computations of the properties of hadron resonances using *lattice* QCD. Evidence for highly excited D mesons has been obtained, including patterns of states beyond the quark model with apparent gluonic content [26–28]. These methods are able to determine the scattering amplitudes and their spectroscopic content to compare with experiment. Relevant for the axial-vector D_1 mesons, the scattering of hadrons with spin in coupled ${}^3S_1$-${}^3D_1$ amplitudes was first studied in a weakly interacting system [29] and later in the context of

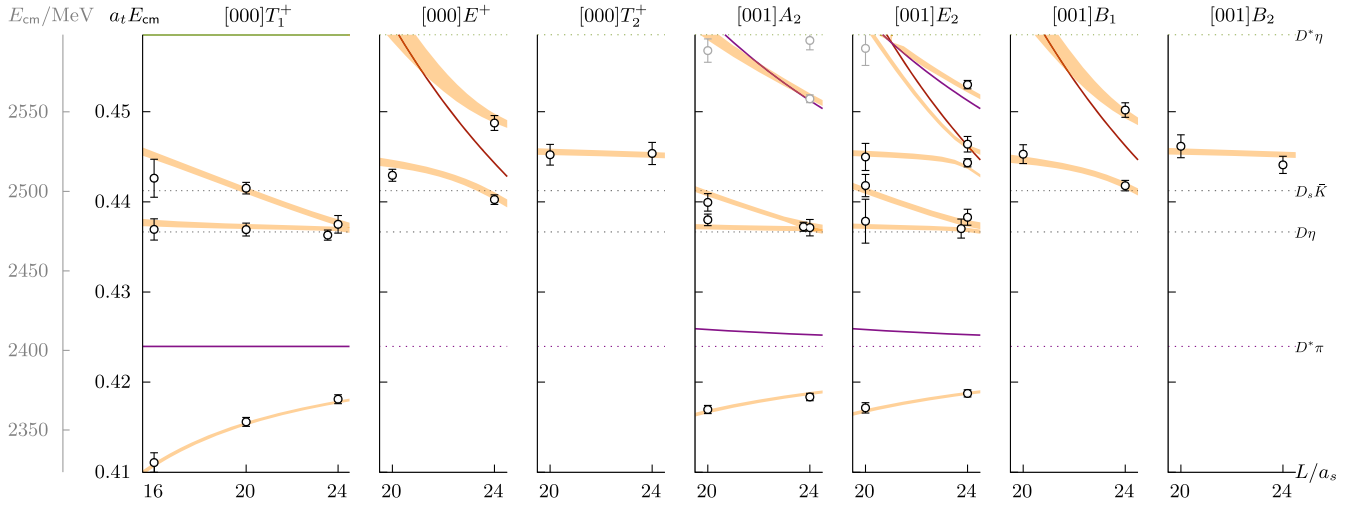

FIG. 1. The black and gray points show the finite volume spectra obtained from irreps up to $|\vec{P}| = 1$ that contain $J^P \in \{1^+, 2^+\}$. Only black points are used in the fit. The thin solid curves show the spectrum anticipated in the absence of interactions between $D^*\pi$ (purple), $D\pi$ (red), and $D^*\eta$ (green). Dotted lines represent kinematic meson-meson thresholds. The $D\pi$ threshold lies below the displayed energy range. The light yellow bands correspond to solutions of the determinant condition [Eq. (1)] using the described parametrization. Additional irreps are shown in the Supplemental Material, Sec. A [64].

the b_1 resonance [30]. The scalar charmed resonances have been investigated in both the charm-light [18,31,32] and charm-strange [33–38] flavors. A large coupling to the strong-decay channels was found in both cases. The axial vectors were also studied in Refs. [31,35,36].

In this Letter, we determine the D_1 masses and couplings to $I = 1/2$ $D^*\pi$ scattering from QCD. We also compute the D_2^* and its couplings to both $D^*\pi$ and $D\pi$ decay modes. With the D_0^* determined from the same lattices [18,32], we compare these states to experiment and probe the predictions from the heavy-quark limit.

Computing finite-volume spectra.—Lattice QCD is a numerical approach through which first-principles predictions of strongly coupled QCD can be obtained by Monte Carlo sampling the QCD path integral. Working in a discretized finite Euclidean volume $L^3 \times T$ with spatial and temporal lattice spacings a_s and a_t, correlation functions can be computed that determine the QCD spectrum in that volume.

The rotational symmetry of the finite cubic spatial boundary differs from an infinite volume. At rest, we compute spectra within irreducible representations (irreps) of the finite cubic group, rather than the continuous orthogonal group. This results in a linear combination of multiple partial waves of definite J^P within each irrep. Amplitudes grow at threshold with $k^{2\ell}$ which commonly suppresses all but the lowest few partial waves at low energies. We also consider nonzero overall momentum $\vec{P} = (2\pi/L)(i, j, k) = [ijk]$, where the symmetry is further reduced; notably, partial waves with both parities are present in the corresponding irreps. The partial waves contributing to the irreps used in this calculation are described in Ref. [29]. Irreps are labeled by $[ijk]\Lambda^{(P)}$.

We use lattices with $2 + 1$ dynamical flavors of quark, where the strange quark is approximately physical and the light quark produces a pion with $m_\pi \approx 391$ MeV. The ratio of the spatial and temporal lattice spacings on this anisotropic lattice is $a_s/a_t \approx 3.5$ [39,40]. We use three volumes with $(L/a_s)^3 \times T/a_t = \{16^3, 20^3, 24^3\} \times 128$. The scale is estimated using the Ω baryon [41]. This corresponds to $a_s \approx 0.12$ fm, resulting in physical volumes between $(2\text{ fm})^3$ and $(3\text{ fm})^3$. The distillation approach is used, which both enhances signals from the required low energy modes, and allows all of the Wick contractions specified by QCD to be computed efficiently [42]. The charm quark uses the same action as the light and strange quarks [26]. Crucial to this study, the vector D^* is stable at this light-quark mass [27].

The variational method is used to extract spectra from correlation functions [43–45]. Special care is needed in choosing operators with good overlap onto all the states present within the investigated energy range. In this Letter, we use a large basis of approximately local $q\bar{q}$- and meson-meson-like operators. The latter are constructed from pairs of mesons obtained variationally from large bases of $q\bar{q}$-like operators to reduce excited state contributions [46–48]. The correlation functions form a matrix that is diagonalized using a generalized eigenvalue approach. The time dependence of the eigenvalues yields the finite volume spectrum $\{E_{\mathfrak{n}}\}$. These spectra expose the underlying scattering amplitude through Lüscher's finite volume quantization condition, and extensions thereof [49–62]—these methods are reviewed in Ref. [63].

In Fig. 1 we present the finite volume spectra computed in irreps with $\vec{P} = [000]$ and [001] with contributions from $J^P = 1^+$ and 2^+. In $[000]T_1^+$ and $[001]A_2$, we observe three

energy levels below $a_t E = 0.45$ ($\approx$2550 MeV) where only a single energy level would have been expected based on the noninteracting spectrum. This indicates nontrivial interactions in $J^P = 1^+$. The $[000]E^+$ and $[000]T_2^+$ irreps also contain an extra energy level, suggestive of significant $J^P = 2^+$ interactions. Irreps where J^- waves are leading only appear to have small energy shifts in this energy region; additional levels that may correspond to higher resonances are observed to appear at energies well above the region considered here [27]. Further irreps and a list of the operators used are given in the Supplemental Material, Secs. A and B [64].

Scattering amplitude determinations.—The extension of Lüscher's determinant condition for the scattering of hadrons with arbitrary spin can be written [62] as

$$\det[\mathbf{1} + i\boldsymbol{\rho}(E) \cdot \boldsymbol{t}(E) \cdot (\mathbf{1} + i\boldsymbol{\mathcal{M}}(E, L))] = 0, \qquad (1)$$

where E is the cm energy, L is the spatial extent, $\boldsymbol{t}$ is the infinite volume scattering t matrix, and $\boldsymbol{\mathcal{M}}$ is a matrix of known functions of energy, which is dense in partial waves and dependent on the irrep. $\boldsymbol{\rho}$ is a diagonal matrix of phase-space factors. Since $\boldsymbol{t}$ has multiple unknowns at each value of energy, it is necessary to introduce a parametrization. The $J^P = 1^+$ wave can be parametrized using a symmetric 2×2 K matrix, indexed by the $^3S_1$ and $^3D_1$ channel labels. A threshold factor is included to promote the natural threshold behavior of each t-matrix element,

$$t_{ij}^{-1} = (2k_i)^{-\ell_i} K_{ij}^{-1} (2k_j)^{-\ell_j} + I_{ij}, \qquad (2)$$

where k_i are the cm momenta, K_{ij} are the K-matrix elements, and I_{ij} is a diagonal matrix. To respect unitarity, $\mathrm{Im} I_{ij} = -\rho_i \delta_{ij}$, where $\rho_i = 2k_i/E$ are the phase-space factors. The real part is either set to zero or a Chew-Mandelstam phase space is used [65], where a logarithm is generated from the known imaginary part.

One useful form of $\boldsymbol{K}$ is

$$K_{ij} = \sum_{p=1}^{2} \frac{g_{p,i} g_{p,j}}{m_p^2 - s} + \gamma_{ij}. \qquad (3)$$

The K-matrix pole mass m_p and couplings $g_{p,i}$ are free parameters that can efficiently produce resonances in a t matrix. The γ_{ij} form a real symmetric matrix of constants. The free parameters are determined in a χ^2 minimization as defined in Eq. (8) of Ref. [65], to find an amplitude that best describes the finite volume spectra obtained in the lattice calculation. We choose to search for the solutions of Eq. (1) using the eigenvalue decomposition method outlined in Ref. [66], which is ideally suited to problems with multiple channels and partial waves.

We determine the $J^P = (1, 2)^+$ and $(0, 1, 2)^-$ partial waves (everything up to $\ell = 2$) simultaneously from the irreps in Fig. 1, plus $[011]A_2, B_1, B_2$, $[111]A_2, E_2$, and $[002]A_2$, resulting in 94 energy levels ($J^P = 0^+$ does not contribute to any of these irreps). Each wave is parametrized using a version of Eq. (3) with various parameters fixed to zero. For example, for the 1^+ wave we use the poles and the $\gamma_{^3S_1,^3S_1}$ element, and fix the other γ_{ij} to zero. We use a single pole for the 2^+ amplitudes. We find that the J^- waves can be described by simple weakly interacting amplitudes; a constant γ is sufficient in each case. Further details of the parametrization and the parameter values resulting from the χ^2 minimization are given in the Supplemental Material, Sec. C [64]. A $\chi^2/N_{\mathrm{d.o.f.}} = [95.0/(94 - 15)] = 1.20$ is obtained. The spectra from using these amplitudes in Eq. (1) are shown as orange curves in Fig. 1. The amplitudes are plotted in Fig. 2.

The parametrization given in Eq. (3) is one of many reasonable choices. In order to reduce possible bias from a specific choice, we vary the form. We obtain 21 different parametrizations that describe the spectra, summarized in the Supplemental Material, Sec. D [64]. These are used when computing pole positions, couplings, and their uncertainties.

Poles and interpretation.—Scattering amplitude poles describe the spectroscopic content consisting of both unstable resonances and stable bound states. The amplitude is analytically continued to complex s. There is a square-root branch cut beginning at each threshold leading to sheets that can be labeled by the sign of the imaginary part of the momentum in each channel i, $\mathrm{Im} k_i$. Close to a pole, the t matrix is dominated by a term $t_{ij} \sim [c_i c_j/(s_0 - s)]$, where s_0 is the pole position and c_i are the channel couplings.

In the $J^P = 1^+$ amplitudes, we find a bound state close to threshold, strongly coupled to the $^3S_1$ amplitude, that produces a broad enhancement over the energy region where the amplitudes are constrained. The $^3D_1$ amplitude has a coupling to this pole consistent with zero, as shown in the lower left panel of Fig. 3. Because of the proximity of the bound-state pole to threshold, the $k_i^{\ell_i}$ factor severely dampens any $^3D_1$ coupling. The narrow peak in the $^3D_1$ amplitude is produced by a resonance pole dominantly coupled to the $^3D_1$ amplitude, with only a small $^3S_1$ coupling. We find a small but nonzero width in all but two of the parametrizations. Both are rejected due to a larger χ^2 than the rest of the amplitudes; the more subtle case is described further in the Supplemental Material, Sec. E [64].

An additional pole is found at the upper edge of the fitting range close to where the $^3S_1$ amplitude touches zero, as seen in Fig. 2. When a zero occurs on the physical sheet, it is usually accompanied by a pole on an unphysical sheet at a similar energy. Since this pole is so close to both the upper limit of the energy range and the $D^*\eta$ and $D_s^*\bar{K}$

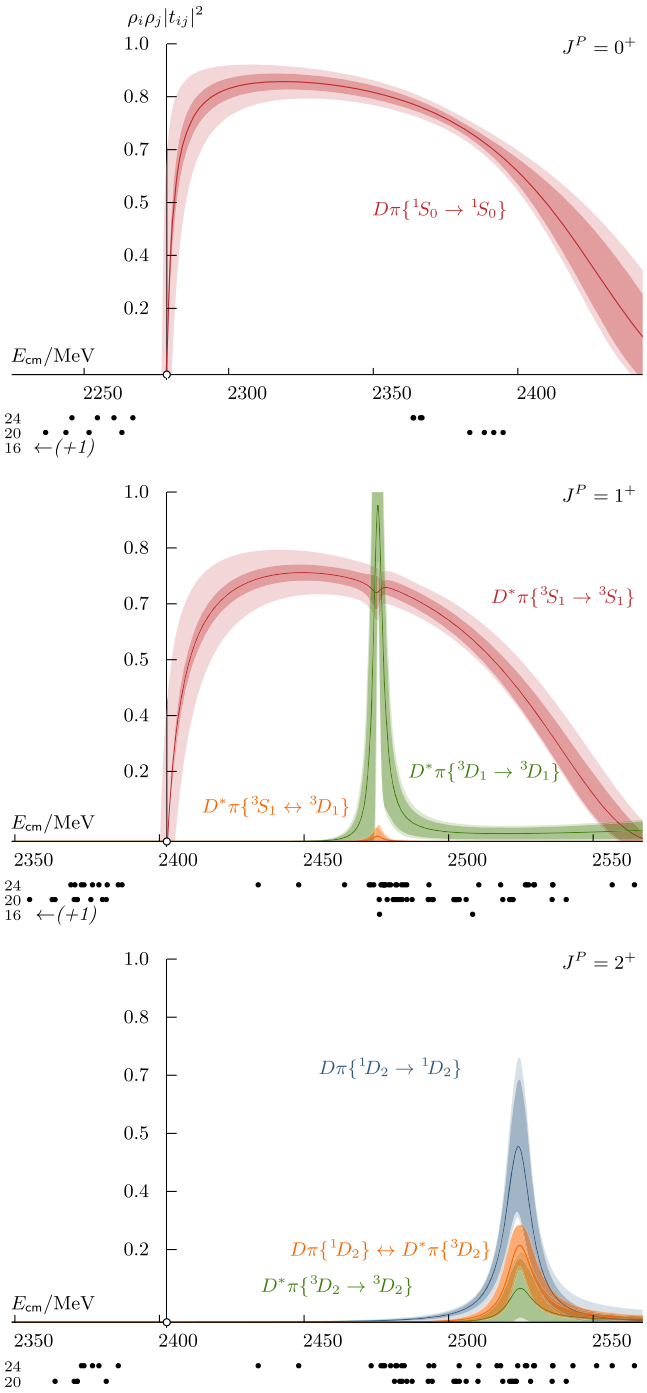

FIG. 2. Scattering amplitudes for $J^P \in \{0^+, 1^+, 2^+\}$. The outer uncertainty bands are obtained by varying the hadron masses and anisotropy entering Eq. (1) within their uncertainties. The energy levels from irreps with a contribution from the respective J^P are shown in black below the horizontal axis. The 0^+ amplitude determination is from Refs. [18,32].

channel openings, higher energy levels are required to be certain of its presence. In one of the rejected amplitudes, this pole does not arise. A similar feature occurs in $D\pi\{^1S_0\}$ elastic scattering that either disappears or moves

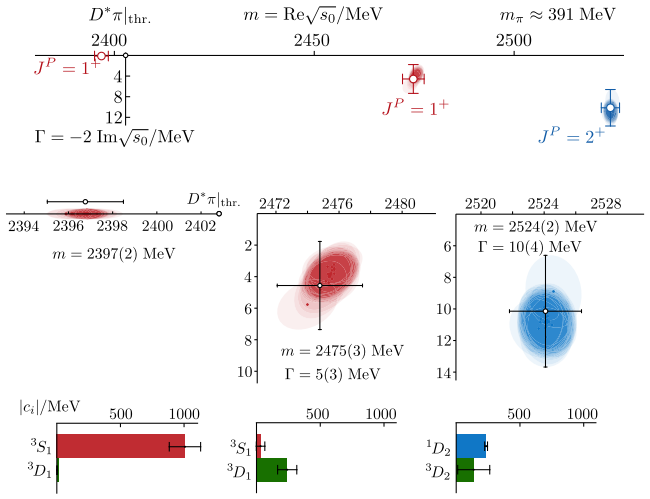

FIG. 3. The t-matrix poles and couplings determined in this study. The top and middle show pole positions; the bottom shows couplings. The colored error ellipses are the results from individual parametrizations and are used to determine the quoted envelope over all parametrizations shown in black.

to higher energies once the coupled-channel $D\eta$ and $D_s\bar{K}$ amplitudes are introduced [32]. We thus exclude this pole from the remaining discussion.

One pole is found in $J^P = 2^+$, coupled to both $D\pi\{^1D_2\}$ and $D^*\pi\{^3D_2\}$. No other nearby poles are found.

In summary, poles are found at

$$\sqrt{s_{D_0^*}} = 2276(2)\ \text{MeV} \qquad (+)\ (\text{from Refs. } [18,32])$$
$$\sqrt{s_{D_1}} = 2397(2)\ \text{MeV} \qquad (+)$$
$$\sqrt{s_{D_1'}} = \left[2475(3) - \frac{i}{2}5(3)\right]\ \text{MeV} \qquad (-)$$
$$\sqrt{s_{D_2^*}} = \left[2524(2) - \frac{i}{2}10(4)\right]\ \text{MeV} \qquad (-,-).$$

The signs in curved brackets indicate the sign of ${\rm Im}k_i$, and thus the sheet where the pole is located. The quoted values correspond to the envelope of uncertainties of all accepted parametrizations as well as mass and anisotropy variations. The couplings are (in MeV)

$$D_0^*: \quad |c_{D\pi\{^1S_0\}}| = 760(164) \qquad (\text{from Refs. } [18,32])$$
$$D_1: \quad |c_{D^*\pi\{^3S_1\}}| = 1007(123) \qquad |c_{D^*\pi\{^3D_1\}}| = 2(3)$$
$$D_1': \quad |c_{D^*\pi\{^3S_1\}}| = 32(33) \qquad |c_{D^*\pi\{^3D_1\}}| = 239(77)$$
$$D_2^*: \quad |c_{D\pi\{^1D_2\}}| = 234(11) \qquad |c_{D^*\pi\{^3D_2\}}| = 137(126).$$

Comparing to experiment, the larger-than-physical light-quark mass must be accounted for. D-meson masses larger than those found in experiment are expected. The D_2^* is found some 80 MeV above the experimental state, and the narrow D_1' is 52 MeV above experiment. The bound-state

pole that produces the broad feature in S wave however is 15 MeV *below* the $D_1(2430)$ found at 2412(9) MeV [5,67]. Considering the similarity of $D\pi\{^1S_0\}$ and $D^*\pi\{^3S_1\}$ along with the light-quark mass dependence of the D_0^* determined in Ref. [18], the broad $D_1(2430)$ could in reality be produced by a pole at a much lower mass. Another difference that arises as the light-quark mass is reduced is that $D\pi\pi$ opens and may introduce more mixing between channels. Recent developments of three-body formalism will be essential in understanding these processes [68–78].

The pole couplings are observed to be relatively insensitive to the quark masses used, both in unitarized chiral amplitudes [79–81] and from lattice calculations [30,82–85], and can thus be used to make connection to experiment. Crudely extrapolating the couplings to lighter pion masses requires a kinematic factor, leading to $|c^{\text{ex.}}| = |c||k^{\text{ex.}}(m_r^{\text{ex.}})/k(m_r)|^\ell$ [82,85]. The D_1' couplings, fixing $m_{D_1'}^{\text{ex.}} = 2422$ MeV [5], produce a consistent width to that observed experimentally, $\Gamma_{D_1'} = 48 \pm 30$ MeV. The D_2^* couplings, fixing $m_{D_2^*}^{\text{ex.}} = 2461$ MeV [5], correspond to $\Gamma_{D_2^*} = 24 \pm 13$ MeV, a little narrower than that observed in experiment. The large coupling found for the bound D_1 suggests this will evolve into a broad resonance as the light-quark mass is reduced [18,86].

Extrapolations in the pion mass have been performed using unitarized chiral amplitudes applied to heavy-light systems by assuming the low-energy constants of the chiral expansion are independent of the pion mass [11,87,88], in particular Refs. [15–17,89,90] that consider the same masses used in this lattice QCD calculation. This method has been demonstrated to work well for the closely related case of S-wave $D\pi$ scattering [15–17], and similar amplitudes exist for the $J^P = 1^+ {}^3S_1$ component [10,19,87].

D^*K in $I = 0$ is related to $D^*\pi$ in $I = 1/2$ by SU(3) flavor symmetry [15,38] and has similarities. The experimental axial-vector D_{s1} hadron masses follow a similar pattern to that observed here, with one bound state and one narrow resonance. The bound state is significantly more bound, and the resonance is narrower. Evidence of a bound D_{s1} was also found in other lattice studies [35,36].

Heavy-quark limit comparisons.—The heavy-quark limit (as described in Refs. [7,14,20–24]) captures many of the features observed in these states. Notably, the prediction of decoupling between the two 1^+ states is upheld in our results. We could not rule out a $^3S_1$ component in the narrow D_1' resonance; many of the parametrizations favor a small but nonzero coupling. The $D\pi\{^1S_0\}$ and $D^*\pi\{^3S_1\}$ amplitudes are remarkably similar in terms of both singularities and energy dependence, producing near-threshold bound states strongly coupled to the relevant nearby channel. Binding energies are found to be 2(1) MeV and 6(2) MeV respectively. Heavy-quark symmetry can also be used to relate the couplings of the narrow D_1' and D_2^*. The results found here are not inconsistent with expectations from the heavy-quark limit; a proper test needs a more precise determination of the couplings, in particular $c_{D^*\pi\{^3D_2\}}$.

The heavy-quark limit and apparent consistency between $^1S_0$ and $^3S_1$ amplitudes working at this light-quark mass, along with the results of Refs. [17,18], implies a broad D_1 resonance with a pole mass well below 2400 MeV for physical light-quark masses.

Summary.—The dynamically coupled $^{2S+1}\ell_J = {}^3S_1$ and $^3D_1$ $D^*\pi$ scattering amplitudes in $I = 1/2$ have been computed from QCD for the first time. Working at $m_\pi \approx 391$ MeV, the $D^*\pi\{^3S_1\}$ amplitude is dominated by a pole just below threshold, whose influence extends over a broad energy region. This pole is found below the experimental state despite the larger pion mass, analogous to the scalar sector. There is a narrow resonance coupled dominantly to the $D^*\pi\{^3D_1\}$ amplitude. The $D^*\pi\{^3S_1\} \to D^*\pi\{^3D_1\}$ amplitude is consistent with zero in the constrained energy region.

The importance of understanding S-wave interactions between pairs of hadrons in QCD cannot be understated. The strength of interactions observed here between a vector and a pseudoscalar not only extends our understanding of D-meson decays; it may point toward a resolution of some of the many other puzzles found with interacting charmed hadrons.

We thank our colleagues within the Hadron Spectrum Collaboration. D. J. W. acknowledges support from a Royal Society University Research Fellowship. D. J. W. acknowledges support from the U.K. Science and Technology Facilities Council (STFC) [Grant No. ST/T000694/1]. The software codes CHROMA [91], QUDA [92,93], QPHIX [94], and QOPQDP [95,96] were used to compute the propagators required for this project. This work used the Cambridge Service for Data Driven Discovery (CSD3), part of which is operated by the University of Cambridge Research Computing Service on behalf of the STFC DiRAC HPC Facility. The DiRAC component of CSD3 was funded by BEIS capital funding via STFC capital Grants No. ST/P002307/1 and No. ST/R002452/1 and STFC operations Grant No. ST/R00689X/1. Other components were provided by Dell EMC and Intel using Tier-2 funding from the Engineering and Physical Sciences Research Council (capital Grant No. EP/P020259/1). This work also used clusters at Jefferson Laboratory under the USQCD Initiative and the LQCD ARRA project, and the authors acknowledge support from the U.S. Department of Energy, Office of Science, Office of Advanced Scientific Computing Research and Office of Nuclear Physics, Scientific Discovery through Advanced Computing (SciDAC) program, and the U.S. Department of Energy Exascale Computing Project. This research was supported in part under an ALCC award, and used resources of the Oak Ridge Leadership Computing Facility at the Oak

Ridge National Laboratory, which is supported by the Office of Science of the U.S. Department of Energy under Contract No. DE-AC05-00OR22725. This research is also part of the Blue Waters sustained-petascale computing project, which is supported by the National Science Foundation (Awards No. OCI-0725070 and No. ACI-1238993) and the state of Illinois. Blue Waters is a joint effort of the University of Illinois at Urbana-Champaign and its National Center for Supercomputing Applications. This work is also part of the PRAC "Lattice QCD on Blue Waters." This research used resources of the National Energy Research Scientific Computing Center (NERSC), a DOE Office of Science User Facility supported by the Office of Science of the U.S. Department of Energy under Contract No. DEAC02-05CH11231. The authors acknowledge the Texas Advanced Computing Center (TACC) at The University of Texas at Austin for providing HPC resources that have contributed to the research results reported within this paper. Gauge configurations were generated using resources awarded from the U.S. Department of Energy INCITE program at Oak Ridge National Lab, NERSC, the NSF Teragrid at the Texas Advanced Computer Center and the Pittsburgh Supercomputer Center, as well as at Jefferson Lab.

*nicolas.lang@maths.tcd.ie
†d.j.wilson@damtp.cam.ac.uk

[1] S. K. Choi *et al.* (Belle Collaboration), Phys. Rev. Lett. **91**, 262001 (2003).
[2] R. Aaij *et al.* (LHCb Collaboration), Sci. Bull. **65**, 1983 (2020).
[3] R. Aaij *et al.* (LHCb Collaboration), Phys. Rev. Lett. **125**, 242001 (2020).
[4] R. Aaij *et al.* (LHCb Collaboration), Phys. Rev. D **102**, 112003 (2020).
[5] P. A. Zyla *et al.* (Particle Data Group), Prog. Theor. Exp. Phys. **2020**, 083C01 (2020).
[6] S. Godfrey and N. Isgur, Phys. Rev. D **32**, 189 (1985).
[7] S. Godfrey and R. Kokoski, Phys. Rev. D **43**, 1679 (1991).
[8] W. A. Bardeen and C. T. Hill, Phys. Rev. D **49**, 409 (1994).
[9] E. van Beveren and G. Rupp, Eur. Phys. J. C **32**, 493 (2004).
[10] E. E. Kolomeitsev and M. F. M. Lutz, Phys. Lett. B **582**, 39 (2004).
[11] J. Hofmann and M. F. M. Lutz, Nucl. Phys. **A733**, 142 (2004).
[12] T. J. Burns, Phys. Rev. D **90**, 034009 (2014).
[13] E. van Beveren and G. Rupp, Phys. Rev. Lett. **91**, 012003 (2003).
[14] W. A. Bardeen, E. J. Eichten, and C. T. Hill, Phys. Rev. D **68**, 054024 (2003).
[15] M. Albaladejo, P. Fernandez-Soler, F.-K. Guo, and J. Nieves, Phys. Lett. B **767**, 465 (2017).
[16] M.-L. Du, M. Albaladejo, P. Fernández-Soler, F.-K. Guo, C. Hanhart, Ulf.-G. Meißner, J. Nieves, and D.-L. Yao, Phys. Rev. D **98**, 094018 (2018).
[17] M.-L. Du, F.-K. Guo, C. Hanhart, B. Kubis, and Ulf.-G. Meißner, Phys. Rev. Lett. **126**, 192001 (2021).
[18] L. Gayer, N. Lang, S. M. Ryan, D. Tims, C. E. Thomas, and D. J. Wilson (Hadron Spectrum Collaboration), J. High Energy Phys. 07 (2021) 123.
[19] X.-Y. Guo, Y. Heo, and M. F. M. Lutz, Phys. Lett. B **791**, 86 (2019).
[20] A. De Rujula, H. Georgi, and S. L. Glashow, Phys. Rev. Lett. **37**, 785 (1976).
[21] J. L. Rosner, Comments Nucl. Part. Phys. **16**, 109 (1986).
[22] N. Isgur and M. B. Wise, Phys. Rev. Lett. **66**, 1130 (1991).
[23] Ming-Lu, M. B. Wise, and N. Isgur, Phys. Rev. D **45**, 1553 (1992).
[24] S. Godfrey, Phys. Rev. D **72**, 054029 (2005).
[25] P. Colangelo, F. De Fazio, F. Giannuzzi, and S. Nicotri, Phys. Rev. D **86**, 054024 (2012).
[26] L. Liu, G. Moir, M. Peardon, S. M. Ryan, C. E. Thomas, P. Vilaseca, J. J. Dudek, R. G. Edwards, B. Joo, and D. G. Richards (Hadron Spectrum Collaboration), J. High Energy Phys. 07 (2012) 126.
[27] G. Moir, M. Peardon, S. M. Ryan, C. E. Thomas, and L. Liu, J. High Energy Phys. 05 (2013) 021.
[28] G. K. C. Cheung, C. O'Hara, G. Moir, M. Peardon, S. M. Ryan, C. E. Thomas, and D. Tims (Hadron Spectrum Collaboration), J. High Energy Phys. 12 (2016) 089.
[29] A. Woss, C. E. Thomas, J. J. Dudek, R. G. Edwards, and D. J. Wilson, J. High Energy Phys. 07 (2018) 043.
[30] A. J. Woss, C. E. Thomas, J. J. Dudek, R. G. Edwards, and D. J. Wilson, Phys. Rev. D **100**, 054506 (2019).
[31] D. Mohler, S. Prelovsek, and R. M. Woloshyn, Phys. Rev. D **87**, 034501 (2013).
[32] G. Moir, M. Peardon, S. M. Ryan, C. E. Thomas, and D. J. Wilson, J. High Energy Phys. 10 (2016) 011.
[33] L. Liu, K. Orginos, F.-K. Guo, C. Hanhart, and Ulf.-G. Meissner, Phys. Rev. D **87**, 014508 (2013).
[34] D. Mohler, C. B. Lang, L. Leskovec, S. Prelovsek, and R. M. Woloshyn, Phys. Rev. Lett. **111**, 222001 (2013).
[35] C. B. Lang, L. Leskovec, D. Mohler, S. Prelovsek, and R. M. Woloshyn, Phys. Rev. D **90**, 034510 (2014).
[36] G. S. Bali, S. Collins, A. Cox, and A. Schäfer, Phys. Rev. D **96**, 074501 (2017).
[37] C. Alexandrou, J. Berlin, J. Finkenrath, T. Leontiou, and M. Wagner, Phys. Rev. D **101**, 034502 (2020).
[38] G. K. C. Cheung, C. E. Thomas, D. J. Wilson, G. Moir, M. Peardon, and S. M. Ryan (Hadron Spectrum Collaboration), J. High Energy Phys. 02 (2021) 100.
[39] R. G. Edwards, B. Joo, and H.-W. Lin, Phys. Rev. D **78**, 054501 (2008).
[40] H.-W. Lin *et al.* (Hadron Spectrum Collaboration), Phys. Rev. D **79**, 034502 (2009).
[41] R. G. Edwards, N. Mathur, D. G. Richards, and S. J. Wallace (Hadron Spectrum Collaboration), Phys. Rev. D **87**, 054506 (2013).
[42] M. Peardon, J. Bulava, J. Foley, C. Morningstar, J. Dudek, R. G. Edwards, B. Joo, H.-W. Lin, D. G. Richards, and K. J. Juge (Hadron Spectrum Collaboration), Phys. Rev. D **80**, 054506 (2009).
[43] C. Michael, Nucl. Phys. **B259**, 58 (1985).
[44] M. Luscher and U. Wolff, Nucl. Phys. **B339**, 222 (1990).
[45] B. Blossier, M. Della Morte, G. von Hippel, T. Mendes, and R. Sommer, J. High Energy Phys. 04 (2009) 094.

[46] J. J. Dudek, R. G. Edwards, M. J. Peardon, D. G. Richards, and C. E. Thomas, Phys. Rev. D **82**, 034508 (2010).
[47] C. E. Thomas, R. G. Edwards, and J. J. Dudek, Phys. Rev. D **85**, 014507 (2012).
[48] J. J. Dudek, R. G. Edwards, and C. E. Thomas, Phys. Rev. D **86**, 034031 (2012).
[49] M. Luscher, Nucl. Phys. **B354**, 531 (1991).
[50] K. Rummukainen and S. A. Gottlieb, Nucl. Phys. **B450**, 397 (1995).
[51] P. F. Bedaque, Phys. Lett. B **593**, 82 (2004).
[52] C. h. Kim, C. T. Sachrajda, and S. R. Sharpe, Nucl. Phys. **B727**, 218 (2005).
[53] Z. Fu, Phys. Rev. D **85**, 014506 (2012).
[54] L. Leskovec and S. Prelovsek, Phys. Rev. D **85**, 114507 (2012).
[55] M. Gockeler, R. Horsley, M. Lage, U. G. Meissner, P. E. L. Rakow, A. Rusetsky, G. Schierholz, and J. M. Zanotti, Phys. Rev. D **86**, 094513 (2012).
[56] S. He, X. Feng, and C. Liu, J. High Energy Phys. 07 (2005) 011.
[57] V. Bernard, M. Lage, U. G. Meissner, and A. Rusetsky, J. High Energy Phys. 01 (2011) 019.
[58] M. Doring, U. G. Meissner, E. Oset, and A. Rusetsky, Eur. Phys. J. A **48**, 114 (2012).
[59] M. T. Hansen and S. R. Sharpe, Phys. Rev. D **86**, 016007 (2012).
[60] R. A. Briceno and Z. Davoudi, Phys. Rev. D **88**, 094507 (2013).
[61] P. Guo, J. J. Dudek, R. G. Edwards, and A. P. Szczepaniak, Phys. Rev. D **88**, 014501 (2013).
[62] R. A. Briceno, Phys. Rev. D **89**, 074507 (2014).
[63] R. A. Briceno, J. J. Dudek, and R. D. Young, Rev. Mod. Phys. **90**, 025001 (2018).
[64] See Supplemental Material at http://link.aps.org/supplemental/10.1103/PhysRevLett.129.252001 for additional finite volume energy levels, operators tables and amplitude determination details.
[65] D. J. Wilson, J. J. Dudek, R. G. Edwards, and C. E. Thomas, Phys. Rev. D **91**, 054008 (2015).
[66] A. J. Woss, D. J. Wilson, and J. J. Dudek (Hadron Spectrum Collaboration), Phys. Rev. D **101**, 114505 (2020).
[67] R. Aaij *et al.* (LHCb Collaboration), Phys. Rev. D **101**, 032005 (2020).
[68] M. T. Hansen and S. R. Sharpe, Phys. Rev. D **92**, 114509 (2015).
[69] R. A. Briceño, M. T. Hansen, and S. R. Sharpe, Phys. Rev. D **99**, 014516 (2019).
[70] M. T. Hansen and S. R. Sharpe, Annu. Rev. Nucl. Part. Sci. **69**, 65 (2019).
[71] T. D. Blanton and S. R. Sharpe, Phys. Rev. D **102**, 054515 (2020).
[72] T. D. Blanton and S. R. Sharpe, Phys. Rev. D **103**, 054503 (2021).
[73] T. D. Blanton and S. R. Sharpe, Phys. Rev. D **104**, 034509 (2021).
[74] T. D. Blanton, F. Romero-López, and S. R. Sharpe, J. High Energy Phys. 02 (2022) 098.
[75] M. Mai and M. Döring, Eur. Phys. J. A **53**, 240 (2017).
[76] K. Polejaeva and A. Rusetsky, Eur. Phys. J. A **48**, 67 (2012).
[77] H.-W. Hammer, J.-Y. Pang, and A. Rusetsky, J. High Energy Phys. 09 (2017) 109.
[78] H. W. Hammer, J. Y. Pang, and A. Rusetsky, J. High Energy Phys. 10 (2017) 115.
[79] J. Nebreda and J. R. Pelaez, Phys. Rev. D **81**, 054035 (2010).
[80] D. R. Bolton, R. A. Briceno, and D. J. Wilson, Phys. Lett. B **757**, 50 (2016).
[81] R. Molina and J. Ruiz de Elvira, J. High Energy Phys. 11 (2020) 017.
[82] D. J. Wilson, R. A. Briceno, J. J. Dudek, R. G. Edwards, and C. E. Thomas, Phys. Rev. D **92**, 094502 (2015).
[83] R. A. Briceno, J. J. Dudek, R. G. Edwards, and D. J. Wilson, Phys. Rev. D **97**, 054513 (2018).
[84] D. J. Wilson, R. A. Briceno, J. J. Dudek, R. G. Edwards, and C. E. Thomas, Phys. Rev. Lett. **123**, 042002 (2019).
[85] A. J. Woss, J. J. Dudek, R. G. Edwards, C. E. Thomas, and D. J. Wilson (Hadron Spectrum Collaboration), Phys. Rev. D **103**, 054502 (2021).
[86] R. A. Briceno, J. J. Dudek, R. G. Edwards, and D. J. Wilson, Phys. Rev. Lett. **118**, 022002 (2017).
[87] F.-K. Guo, P.-N. Shen, and H.-C. Chiang, Phys. Lett. B **647**, 133 (2007).
[88] D. Gamermann, E. Oset, D. Strottman, and M. J. Vicente Vacas, Phys. Rev. D **76**, 074016 (2007).
[89] F.-K. Guo, C. Hanhart, Ulf.-G. Meißner, Q. Wang, Q. Zhao, and B.-S. Zou, Rev. Mod. Phys. **90**, 015004 (2018); **94**, 029901(E) (2022);.
[90] X.-Y. Guo, Y. Heo, and M. F. M. Lutz, Phys. Rev. D **98**, 014510 (2018).
[91] R. G. Edwards and B. Joo, Nucl. Phys. B, Proc. Suppl. **140**, 832 (2005).
[92] M. A. Clark, R. Babich, K. Barros, R. C. Brower, and C. Rebbi, Comput. Phys. Commun. **181**, 1517 (2010).
[93] R. Babich, M. A. Clark, and B. Joo, in *SC '10: Proceedings of the 2010 ACM/IEEE International Conference for High Performance Computing, Networking, Storage and Analysis, New Orleans, LA* (IEEE, New York,), 10.1109/SC.2010.40.
[94] B. Joó, D. D. Kalamkar, K. Vaidyanathan, M. Smelyanskiy, K. Pamnany, V. W. Lee, P. Dubey, and W. Watson, Lect. Notes Comput. Sci. **7905**, 40 (2013).
[95] J. C. Osborn, R. Babich, J. Brannick, R. C. Brower, M. A. Clark, S. D. Cohen, and C. Rebbi, Proc. Sci., LATTICE2010 (**2010**) 037.
[96] R. Babich, J. Brannick, R. C. Brower, M. A. Clark, T. A. Manteuffel, S. F. McCormick, J. C. Osborn, and C. Rebbi, Phys. Rev. Lett. **105**, 201602 (2010).